LINGERING GRAINS OF TRUTH AROUND COMET 17P/HOLMES

R. Stevenson[1], J. M. Bauer[1,2], E. A. Kramer[3], T. Grav[4], A. K. Mainzer[1], and J. R. Masiero[1]

[1] Jet Propulsion Laboratory, California Institute of Technology, 4800 Oak Grove Drive,
MS 183-427, Pasadena, CA 91109, USA; Rachel.A.Stevenson@jpl.nasa.gov
[2] Infrared Processing and Analysis Center, California Institute of Technology, Pasadena, CA 91125, USA
[3] Department of Physics, University of Central Florida, 4000 Central Florida Blvd, Orlando, FL 32816, USA
[4] Planetary Science Institute, 1700 East Fort Lowell, Suite 106, Tucson, AZ 85719-2395, USA

ABSTRACT

Comet 17P/Holmes underwent a massive outburst in 2007 October, brightening by a factor of almost a million in under 48 hr. We used infrared images taken by the *Wide-Field Infrared Survey Explorer* mission to characterize the comet as it appeared at a heliocentric distance of 5.1 AU almost 3 yr after the outburst. The comet appeared to be active with a coma and dust trail along the orbital plane. We constrained the diameter, albedo, and beaming parameter of the nucleus to 4.135 ± 0.610 km, 0.03 ± 0.01, and 1.03 ± 0.21, respectively. The properties of the nucleus are consistent with those of other Jupiter family comets. The best-fit temperature of the coma was 134 ± 11 K, slightly higher than the blackbody temperature at that heliocentric distance. Using Finson–Probstein modeling, we found that the morphology of the trail was consistent with ejection during the 2007 outburst and was made up of dust grains between 250 μm and a few cm in radius. The trail mass was ~ 1.2–5.3×10^{10} kg.

Key words: comets: general – comets: individual (17P/Holmes)

Online-only material: color figures

1. INTRODUCTION

Comet 17P/Holmes (hereafter 17P) has undergone three massive outbursts since its discovery in 1892 (Holmes 1892), most recently brightening by a factor of almost a million and becoming visible to the naked eye in 2007 October. The outbursts are likely thermally driven, since all three occurred six to nine months after 17P passed through perihelion. Dynamically, 17P appears to be a typical Jupiter family comet (JFC) with a semimajor axis of 3.62 AU, eccentricity of 0.43, and inclination of 19°.1. The comet is enigmatic given its propensity for unusually large outbursts, but has dynamical and physical properties similar to other JFCs.

The material ejected during the 2007 outburst included gas species, dust grains, and macroscopic fragments (e.g., Dello Russo et al. 2008; Crovisier et al. 2009; Yang et al. 2009; Reach et al. 2010; Stevenson et al. 2010). Much of the smaller dust expanded in an almost spherical shell around the nucleus, while larger dust grains were observed to separate as a "blob" at a slower rate of $\sim$120–135 m s^{-1} (e.g., Montalto et al. 2008; Lin et al. 2009; Hsieh et al. 2010). Reach et al. (2010) and Boissier et al. (2012) detected a slower moving core-component of the largest grains that separated from the nucleus at a relative velocity of $\sim$7–9 m s^{-1}. Large dust grains may persist in the vicinity or along the trail of a comet for years after ejection from the nucleus (Sykes et al. 1990; Lisse et al. 1998; Bauer et al. 2011). In this work we used infrared (IR) images obtained with the *Wide-Field Infrared Survey Explorer* (*WISE*) to examine the evolution of 17P several years after the 2007 outburst.

2. *WISE* OBSERVATIONS AND REDUCTION

The *WISE* telescope launched in 2009 December and conducted an all-sky survey over the following year. The 40 cm telescope simultaneously covered a $47' \times 47'$ field of view in four IR bands. The bands had central wavelengths of 3.4 μm, 4.6 μm, 12 μm, and 22 μm, and are referred to as $W1$, $W2$, $W3$, and $W4$, respectively. The median pixel scale in bands $W1$, $W2$, and $W3$ was 2″.8 pixel^{-1}, whereas 2×2 binned $W4$ images had a pixel scale of 5″.5 pixel^{-1} (Wright et al. 2010). The effective exposure times were 7.7 s for $W1$ and $W2$ images, and 8.8 s for $W3$ and $W4$ images. The individual exposures and extracted sources from each frame were archived and searched using tools developed as part of the NEOWISE project (Mainzer et al. 2011).

The data were initially processed by the *WISE* Science Data System, which removed the instrumental signatures and provided astrometric and photometric calibration. Astrometric accuracy was $\sim$0″.2, while absolute photometric accuracy was $\sim$5%–10% (Mainzer et al. 2011; Cutri et al. 2012).

WISE pointed toward 17P a total of 14 times during the mission. Three of these sets of images were obtained after the cryogen had been depleted and thus only produced images at the two shortest wavelengths. Here we use the 11 sets of images in all four bands that were obtained within 24 hr between UT 2010 May 14 and 15 (Table 1). At this time 17P was at a heliocentric distance of 5.1 AU and a true anomaly of $\sim$170°, which is approximately five months prior to reaching aphelion. These frames were aligned using the predicted orbital motion of the comet as calculated by the JPL Horizons ephemeris service and combined using the AWAIC (A *WISE* Astronomical Image Co-adder) stacking algorithm (Masci & Fowler 2009), which includes an outlier-rejection algorithm. By using the stacked images for this work, we increased the signal-to-noise ratio, and average over rotational variations, which may amount to 0.3 mag in R band (Snodgrass et al. 2006). The stacked images were resampled to have pixel scales of 1″ pixel^{-1}, corresponding to a projected on-sky distance of 3600 km pixel^{-1}, with pointspread functions (PSFs) having average FWHM of 6″.1, 6″.4, 6″.5, and 12″.0 in bands $W1$, $W2$, $W3$, and $W4$, respectively (Wright et al. 2010). Although the spacecraft did not track the comet's motion, trailing is not a concern since the maximum motion of the comet during an exposure was 0″.03, significantly less than the FWHM or pixel scale of any image.
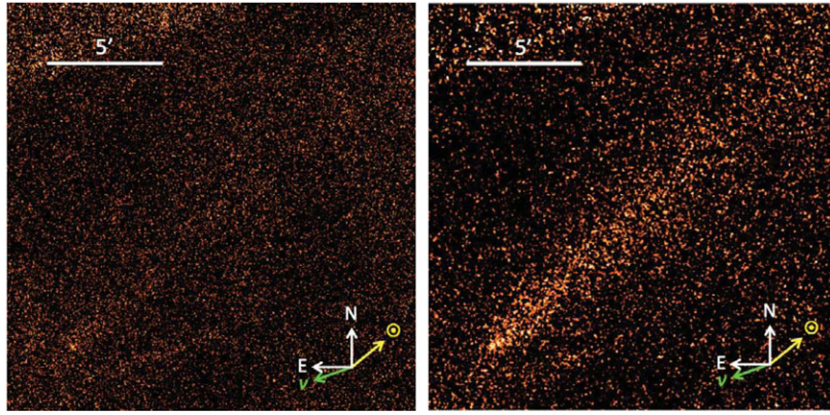
Figure 1. Comet 17P/Holmes as observed by the *WISE* mission in *W*3 (left; 12 μm) and *W*4 (right; 22 μm) on UT 2010 May 14 and 15. The nucleus is located in the southeast corner of the image. Celestial north (N) and east (E) are marked, as are the solar ($\odot$) and velocity (v) vectors.

(A color version of this figure is available in the online journal.)

Table 1
Observations

	Date (UT)	Number of Frames	r_H (AU)	Δ (AU)	α (deg)
17P/Holmes	2010 May 14–15	11	5.13	4.93	11.3

Table 2
Fluxes in mJy

	*W*1 (3.4 μm)	*W*2 (4.6 μm)	*W*3 (12 μm)	*W*4 (22 μm)
17P/Holmes, total flux	<0.03	<0.10	0.77 ± 0.15	8.97 ± 1.91
Nucleus (measured)	<0.03	<0.10	0.33 ± 0.05	1.56 ± 0.31
Nucleus (best-fit)	1.92×10^{-4}	2.04×10^{-4}	0.27	1.68
Coma (measured)	<0.03	<0.10	0.45 ± 0.09	7.41 ± 1.58
Coma (best-fit)	5.91×10^{-3}	3.59×10^{-3}	0.45	7.41

To convert counts to fluxes we used the instrumental zero points given in Wright et al. (2010). We revised the zero points by −8% in *W*3 and +4% in *W*4 to account for the observed discrepancy between the red and blue calibrators. We corrected for the loss of light outside fixed apertures by using the aperture corrections given in Cutri et al. (2011). These amounted to −0.34 and −0.65 mag for *W*3 and *W*4 for apertures of radius 11″. In this work, we chose to use apertures with radii of 11″ as a compromise between limiting the intrusion of background signal into the aperture and still capturing the majority of the PSF. Finally, we performed a color correction, which was necessary due to the wide band pass of the filters. We calculated the correction by interpolating the color corrections given for a range of temperatures in Wright et al. (2010) to the estimated blackbody temperature of 17P.

3. RESULTS

17P was detected in the longer wavelength *W*3 and *W*4 bands (Figure 1), but was not detected in bands *W*1 or *W*2. A dust trail was seen in both *W*3 and *W*4 images, although it was considerably brighter in *W*4. The modal average of the background was calculated ∼5′ from the nucleus over an area of ∼2.2 arcmin^2 and was subtracted from the stacked images. We set 5σ upper limits on the signal from 17P in the *W*1 and *W*2 bands of 0.03 mJy and 0.10 mJy, respectively, using an 11″ radius aperture. The total fluxes within the 11″ radius apertures were 0.77 ± 0.15 mJy and 8.97 ± 1.91 mJy in bands *W*3 and *W*4, respectively. Table 2 shows the fluxes measured for 17P and the fluxes obtained by best-fit thermal models to the nucleus and coma signals (discussed in Sections 3.1 and 3.2, respectively).

3.1. Nucleus

The total signal was a mix of contributions from the nucleus and dust particles in the coma and trail around the nucleus. We separated those signals by fitting the non-PSF-like signal with an analytical function of the form $F\rho^{-n}$, where F is a scalar, ρ is the distance from the nucleus, and n is a power law index (Fernández 1999; Lisse et al. 1999). This model was

centered on the nucleus and fitted for 120 azimuthal slices, each 3° in azimuth. We assumed that the coma behavior is constant near the nucleus and is well modeled by a power law. We experimented with a range of annuli of varying positions and varying widths. The best fit was identified by examining the remaining "nucleus" signal and comparing its shape to a model PSF for the *WISE* images using a least-squares minimization technique. We elected to use annuli fitted between the nucleo-centric distances of 11″ and 14″ for the *W*3 image, and 13″ and 29″ for the *W*4 image. The model of the coma was then subtracted, leaving the nucleus signal behind. The remaining nucleus signal is compared to the model PSF in Figure 2.

We used aperture photometry to investigate the extracted nucleus signal. The aperture was centered on the position of the nucleus as predicted by the JPL Horizons service. The signal from the nucleus was 0.33 ± 0.05 mJy and 1.56 ± 0.31 mJy in *W*3 and *W*4, respectively.

The *W*3 and *W*4 signals were fit to a near-Earth Asteroid Thermal Model (NEATM; Harris 1998). The model assumes that the nucleus is spherical and acts as a smooth Lambertian surface (Cruikshank & Jones 1977; Brown 1985). We assumed that the emissivity of the surface was 0.9, consistent with refractory materials (Lebofsky et al. 1986). The free-fit parameters were diameter (D) and beaming parameter (η). The best-fit results were $D = 4.135 \pm 0.610$ km, $\eta = 1.03 \pm 0.21$. We adopted the absolute magnitude of the nucleus to be $H = 16.24 \pm 0.02$ as determined by Snodgrass et al. (2006) when the comet appeared to be inactive in 2005. By coupling the absolute magnitude to the thermal fit we derive the albedo to be $p_v = 0.03 \pm 0.01$.

3.2. Coma

We used aperture photometry to investigate the dust coma. We subtracted the extracted nucleus signal reported in Section 3.1 from the results, giving coma fluxes of 0.45 ± 0.09 mJy in *W*3
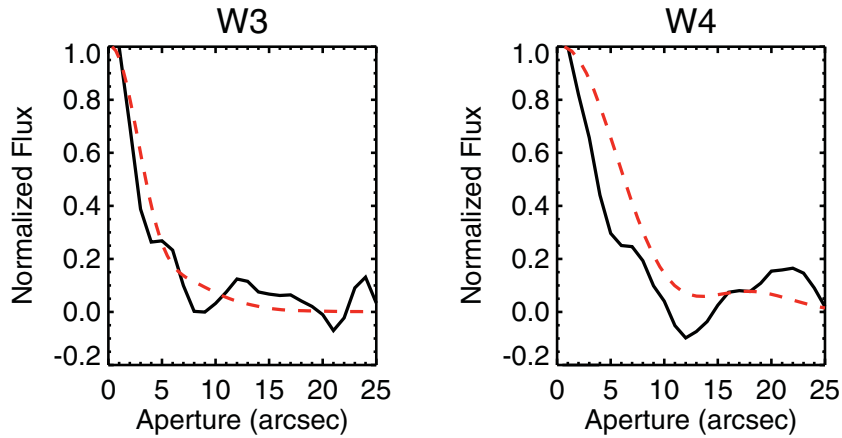
W3

W4

Figure 2. Surface brightness profile of the signal that remained following coma subtraction (black solid line) and the *WISE* PSF (red dashed line) for bands *W*3 (left) and *W*4 (right).

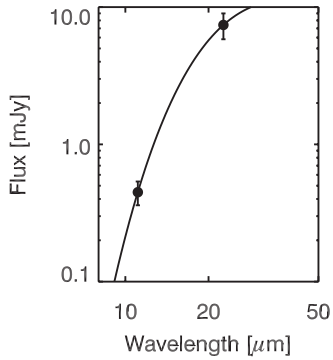(A color version of this figure is available in the online journal.)

Figure 3. Coma temperature fit to signal from the dust coma of 17P/Holmes. The best-fit temperature is 134 ± 11 K, which is ∼10% higher than the local blackbody temperature.

and 7.41 ± 1.58 mJy in *W*4. We assumed that the signal is thermal emission, rather than reflected light, and fitted the data points at thermal wavelengths with a simple blackbody curve to determine the temperature. The best fit is shown in Figure 3 and corresponds to a temperature of 134 ± 11 K, ∼10% higher than the local blackbody temperature.

3.3. Dust Trail

We observed a broad dust trail lagging the nucleus of 17P in the *W*3 and *W*4 images. Given the extremely low surface brightness of the trail in *W*3, we restricted our analyses to the *W*4 data. The trail lay in the orbital plane of 17P and was observed to stretch over 3.1×10^6 km (∼14′.7) as projected on the sky.

In order to determine the best model, the trail shape was first characterized using the following method: (1) using a 40″ annulus centered on the comet, unwrap the image in r–θ space, (2) fit a Gaussian to the unwrapped data across radial bins of 2° width, giving a location that can be converted back to the x–y space, (3) repeat the process along the length of the trail. This process compresses the trail into a series of 21 discrete points that can then be analytically compared to the models described below. Several combinations of annulus width (20″–50″ in steps of 10″) and radial bin size (1°, 2°, and 3°) were considered, with 40″ annuli and 2° radial bins giving the least amount of scatter in the positions.

The dust trail was modeled using the Finson–Probstein method (Finson & Probstein 1968), which assumes that the

motion of cometary dust particles is controlled by solar gravity, F_{grav}, and solar radiation, F_{rad}. The motion can be parameterized using the ratio of the two forces, β:

$$\beta = \frac{F_{\mathrm{rad}}}{F_{\mathrm{grav}}} = \frac{5.76 \times 10^{-4} Q_{\mathrm{pr}}}{\rho_d a_d}, \qquad (1)$$

where Q_{pr} is the scattering efficiency, ρ_d is the density of the particle (kg m^{-3}), and a_r is the particle radius (m). For grains with radii larger than the wavelength of observations, Q_{pr} is approximately equal to 1 (Burns et al. 1979). Thus, β depends on the inverse of particle diameter, that is, for smaller grains, β is larger, meaning the radiation pressure pushing the particles outward has a larger effect than the gravitational force pulling them inward. We integrated the motion of the dust particles over a period of 5 yr. This generated a set of points that can be shown as curves of constant radius particles released at a range of times (syndynes) or curve of constant release date with a range of particle radii (synchrones).

For both the syndynes and synchrones, we calculated the rms between each model and the fitted tail points. The lowest rms value for any of the syndynes is higher than for any of the synchrones, thus we proceeded to fit the trail with a synchrone. The synchrone with the lowest rms to the fitted trail points was determined to correspond to the best-fit particle ejection date. To constrain the error on the best-fit date, we computed the best-fit synchrone for each fitted point along the trail and computed the rms between those synchrones and the overall best-fit synchrone. This analysis yielded a best-fit ejection date of 2007 October 27 $\pm$ 221 days. The large error bars are due to some of the fitted trail points deviating significantly from the best-fit synchrone, and thus giving dramatically different best-fit ejection dates. Example syndynes and synchrones, as well as the best fit, are plotted in Figure 4. It is possible that some of the largest grains were released on previous perihelion passages as Reach et al. (2010) observed an old debris trail along the orbit of 17P using the *Spitzer Space Telescope* in 2008. However, the contribution is likely negligible given the good fit by the synchrone analysis.

The surface brightness of the trail was too low to estimate the size distribution of particles along its length, although we can set the minimum radius of observed particles to ∼250 μm. This is done by finding the syndyne that crosses the trail near the observed edge (14′.3 from the nucleus). Using the same method,
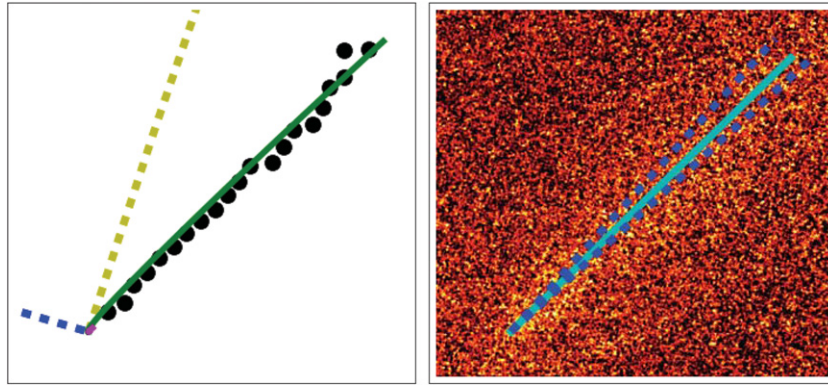
Figure 4. Left: schematic showing the fitted trail (black points) with two example synchrones in blue and yellow dashed lines, corresponding to particle ejection dates of six months and 1 yr prior to observation, respectively. The solid green and magenta lines are the syndynes for particles of diameter 250 μm and 3 cm located at the apparent end of the trail and 11″ from the nucleus, respectively. Right: the dust trail of 17P with the best fit synchrone and error bars overplotted. The best fit corresponds to dust that was ejected on 2007 October 27 $\pm$ 221 days.

(A color version of this figure is available in the online journal.)

we estimate that particles near ($\sim$11″ from) the nucleus are on the order of a few centimeters in diameter. Smaller particles likely existed beyond the trail observed by *WISE*, but are below the detection limit.

4. DISCUSSION

4.1. Physical Properties of the Nucleus

The effective nucleus diameter of 4.135 ± 0.610 km calculated here is larger than previous estimates of 3.24 ± 0.02 km (Snodgrass et al. 2006) and 3.42 ± 0.14 km (Lamy et al. 2009), which were derived when 17P appeared to be inactive or only weakly active prior to its 2007 outburst. Both of the previously mentioned results were determined from optical observations using an assumed albedo of 0.04. The diameter reported here is consistent with previously reported results once corrected using the NEOWISE-derived albedo.

We derived an albedo of 0.03 ± 0.01. The albedo of the nucleus is consistent with those measured for other comets, which generally occupy a narrow range between 0.02 and 0.06 (Lamy et al. 2004). We note that we are unable to derive an albedo for material in the trail as we do not have simultaneous high signal-to-noise observations at optical wavelengths. Ishiguro et al. (2010) used optical, near-IR, and mid-IR observations to constrain the albedo of the ejecta within a few days of the outburst. They found that the albedo of the material (as observed at a phase angle of 16°) decreased during their observations from 0.12 ± 0.04 to 0.032 ± 0.014 and suggested that sublimating volatiles would lower the albedo. Lacerda & Jewitt (2012) estimated the geometric albedo of the dust in the coma as 0.006 ± 0.002, also at a phase angle of 16°. Such a low value is not unheard of (Soderblom et al. 2002; Nelson et al. 2004), although it does not match well with results from Ishiguro et al. (2010). The discrepancy may be due to different populations of grains dominating the thermal emission in the IR and the stellar extinction at optical wavelengths. Our result for the albedo of the nucleus is generally consistent with the albedo of the ejecta observed in 2007, when the albedo was determined from combined optical and mid-IR wavelengths.

The beaming parameter of 1.03 ± 0.21 is consistent with the average value of 1.03 ± 0.11 reported for 57 JFCs by the SePPCoN survey, which used thermal infrared measurements by the *Spitzer Space Telescope* (Fernández et al. 2013). They found

that beaming parameters for 57 JFC nuclei were approximately normally distributed and suggested that there appears to be little variation among bulk thermal properties of JFCs. As discussed in Fernández et al. (2013), a beaming parameter close to 1.0 implies low thermal inertia and little nightside emission. 17P appears typical in this regard.

4.2. Thermal Emission in the Coma

The best-fit coma temperature of 134 ± 11 K is $\sim$10% warmer than the temperature expected for an ideal blackbody (T_{BB}) at a heliocentric distance of 5.13 AU (123 K assuming $T_{\mathrm{BB}} \propto 278$ K $r_{\mathrm{H}}^{-0.5}$; Gehrz & Ney 1992). Previous results from observations taken close to the time of outburst ($r_{\mathrm{H}} \sim$ 2.4 AU) have also suggested that the dust temperature of the ejecta exceeded the local blackbody temperature of $\sim$180 K. Yang et al. (2009) reported a dust temperature near the nucleus of 360 ± 40 K using near-IR observations obtained with the NASA Infrared Telescope Facility several days after the outburst, whereas mid-IR results obtained around the same time suggested cooler temperatures between 172 K and 200 K (Ishiguro et al. 2010; Watanabe et al. 2009). *Spitzer Space Telescope* observations obtained on 2007 November 10 resulted in an estimated temperature of 260 K for the near-nucleus dust (Reach et al. 2010). Most of these results are higher than the estimated blackbody temperature to varying degrees, matching well with our results here.

Numerous IR observations of comets have shown that it is common, perhaps even the norm, for comae and dust tail and trail temperatures to exceed the temperature expected for a co-located blackbody (e.g., Tokunaga et al. 1988; Gehrz & Ney 1992; Lisse et al. 1998; Hayward et al. 2000). Generally, excess emission at IR wavelengths is attributed to either small grains ($\lesssim$1 μm) that are unable to radiate efficiently at IR wavelengths, rough surfaced grains that are more emissive than the smooth spherical grains modeled by the blackbody temperature, or larger grains that maintain a thermal gradient across their surface (Campins & Hanner 1982; Sykes et al. 1990; Sekanina et al. 2001). In the case of 17P, all these effects may be present. The nucleus was seen to remain active in the months and years following the outburst, likely releasing small dust grains from the surface (Stevenson & Jewitt 2012; C. Snodgrass 2013, private communication). Based on results from the best-fit synchrone determined in Section 3.3, particles larger than a few

centimeters in diameter would still be close enough to the nucleus to contribute to the excess thermal emission observed here.

4.3. An Old Trail

The morphology of the trail is consistent with being debris ejected during the 2007 outburst and observations by Ishiguro et al. (2013) that showed large dust grains following the comet around aphelion in 2010 October. We constrained the range of particle diameters observed between ∼250 μm and a few cm. The larger grain diameters are consistent with the size of the grains observed in a slow-moving "core" near the nucleus just a few days after the outburst, which were determined to be $\gtrsim$200 μm (Reach et al. 2010; Boissier et al. 2012).

We measured the flux along the trail using a box aperture that extends between 11″ and 880″ from the nucleus and has a width perpendicular to the length of the trail of 52″. The flux was calibrated and color-corrected as described in Section 2. To correct for light potentially lost outside the large aperture, we applied an aperture correction of −0.03 mag derived by Jarrett et al. (2013). To estimate the cross-section of material present, we used the following relation from Min et al. (2005):

$$\sigma_\lambda = \frac{F_\lambda \Delta^2}{B_\lambda(T)}, \tag{2}$$

where σ_λ is the cross-section of material observed at wavelength λ (in this case, 22 μm, or W4), F_λ is the observed flux, Δ is the geocentric distance, and $B_\lambda(T)$ is the Planck function at temperature T. We were unable to constrain the temperature of the dust along the trail as the signal in W3 is too low to fit to a Planck function. We therefore assumed that the temperature is between the expected blackbody temperature of 123 K and the measured coma temperature of 134 K. This is consistent with the previously discussed finding that many comet trails are at or exceed local blackbody temperatures. We also assumed that the temperature is constant along the trail and is not dependent on the size of the dust grains present. The cross-section of material was 1.5×10^9 m^2 in the case of the local blackbody temperature or 10^9 m^2 in the higher temperature case. We used previously measured minimum and maximum particle sizes ($a-$, $a+$) of 250 μm and 3 cm, and assumed that the differential size distribution of particles follows a power law of the form $n(a)da \propto a^{-q}da$, with the value of q set between 2.2 and 3.4, as measured by Reach et al. (2010) and Boissier et al. (2012), respectively. The mean particle size within the trail was given by

$$\bar{a} = \frac{\int_{a-}^{a+} \pi a^3 n(a)da}{\int_{a-}^{a+} \pi a^2 n(a)da}. \tag{3}$$

The mass within the observed trail was then given by

$$M = \frac{4\rho\bar{a}\sigma_\lambda}{3}, \tag{4}$$

where ρ is the bulk density of the grains and was assumed to be 1000 kg m^{-3} (Jewitt 1991). The mass in the trail was ∼1.2–5.3 × 10^{10} kg. This represented approximately 1%–100% of the total ejected mass (Sekanina 2008; Schleicher 2009; Reach et al. 2010; Ishiguro et al. 2010; Li et al. 2011; Boissier et al. 2012).

Assuming an average grain size of 200 μm, Reach et al. 2010 estimated the mass of the slow-moving core seen in 2007 to be ∼4 × 10^9 kg. Boissier et al. 2012 estimated the mass to be significantly higher at ∼0.7–4 × 10^{11} kg by summing

over an estimated particle size distribution with $a_- = 0.1$ μm, $10 < a_+ < 1000$ mm, and $-3.3 < q < -3.0$. Thus, the dust trail observed by WISE represented 3%–75% of the core modeled by Boissier et al. 2012 in 2007.

4.4. Why Did 17P Outburst?

The overarching question, however, remains to be answered—why does 17P undergo massive outbursts when most JFCs experience only mild mass loss? The diameter, beaming parameter, and albedo of the nucleus are similar to those of other JFC nuclei. The volatile species observed shortly after the outburst in 2007 similarly fail to provide any obvious clues about the cause of the outburst. Relative abundances of CN, C_2, C_3, and NH, as well as the isotopic ratios of ^{12}C/^{13}C and ^{14}N/^{15}N in CN and HCN, were similar to those observed for other comets (Bockelée-Morvan et al. 2008; Schleicher 2009). Several species, including C_2H_6, HCN, CH_3OH, and C_2H_2, were enhanced with respect to H_2O although only by a factor of a few (Dello Russo et al. 2008).

The perihelion distance of 17P changed from 2.17 AU in 2000 to 2.05 AU in 2007 following a close encounter with Jupiter. The change resulted in a ∼10% increase in solar insolation at the surface. The small difference may have caused the thermal wave to propagate deeper than on previous perihelion passages, reaching previously unheated pockets of volatiles. A runaway exothermic phase transition of amorphous water ice to crystalline is probably insufficient to cause the outburst (Kossacki & Szutowicz 2010). If supervolatiles such as CO and/or CO_2 are trapped within the amorphous ice and heated sufficiently, the resulting gas production may be able to drive such activity, if the gas can build up sufficient internal pressure (Schleicher 2009; Sekanina 2009; Kossacki & Szutowicz 2011; Hillman & Prialnik 2012).

It is possible that the nucleus of 17P has unusually high tensile strength that allows gas pressure to build up in the interior before releasing the energy in a sudden outburst upon surface failure. Reach et al. (2010) suggested that the nucleus must have a strength between 10–100 kPa in order to have survived the 2007 outburst. However, previous studies of other comets suggest much lower strengths for JFCs. 16P/Brooks 2 and D/1993 F2 (Shoemaker-Levy 9) both underwent tidal splitting during close encounters with Jupiter, leading to estimates of 0.1 kPa and ∼0.38 kPa for the tensile strengths of the nuclei (Sekanina & Yeomans 1985; Sekanina et al. 1998). Based on observations of mini-outbursts, Belton et al. (2008) estimated the strength of the sub-surface material of 9P/Tempel 1 to be not much more than 0.01–0.1 kPa, while A'Hearn et al. (2005) found that the strength of the surface must also be extremely low (<0.065 kPa). Only a few comets have estimated tensile strengths and are not necessarily representative of all JFCs. We note simply that the estimated tensile strength required of 17P is an order of magnitude higher than those estimated for other JFCs.

5. SUMMARY

We used wide-field IR images obtained by the WISE mission in 2010 May to characterize 17P. Years later, 17P still exhibited evidence of the 2007 outburst. Our results suggest that 17P is a JFC with a typical diameter, albedo, and beaming parameter, but atypical outgassing behavior.

1. The diameter, albedo, and beaming parameter of the nucleus of 17P were constrained to values of 4.135 ± 0.610 km,

0.03 ± 0.01, and 1.03 ± 0.21, respectively. The physical and bulk thermal properties of the nucleus appear to be consistent with those of other JFCs.

2. The temperature of the dust near the nucleus was 134 ± 11 K, which is slightly higher than the local blackbody temperature. Possible explanations for the elevated temperature include emission from small sub-micron grains that cannot effectively radiate at IR wavelengths, or contributions from larger dust grains that maintain a temperature gradient across their surface. Both effects may have been present at the time of observation.

3. 17P was observed to have a debris trail in 2010 May. Dynamical modeling of the dust suggests that this was leftover from the massive 2007 outburst. The range of grain diameters observed is 800 μm to a few centimeters. The mass of the trail was estimated at 1.2–5.3 × 10^{10} kg, which represents ∼1%–100% of the total mass ejected during the 2007 outburst.

REFERENCES

A'Hearn, M. F., Belton, M. J. S., Delamere, W. A., et al. 2005, Sci, 310, 258
Bauer, J. M., Walker, R. G., Mainzer, A. K., et al. 2011, ApJ, 738, 171
Belton, M. J. S., Feldman, P. D., A'Hearn, M. F., & Carcich, B. 2008, Icar, 198, 189
Bockelée-Morvan, D., Biver, N., Jehin, E., et al. 2008, ApJL, 679, L49
Boissier, J., Bockelée-Morvan, D., Biver, N., et al. 2012, A&A, 542, A73
Brown, R. H. 1985, Icar, 64, 53
Burns, J. A., Lamy, P. L., & Soter, S. 1979, Icar, 40, 1
Campins, H., & Hanner, M. S. 1982, in IAU Colloq. 61, Comets (A83-13376 03-90), Comet Discoveries, Statistics, and Observational Selection, ed. L. L. Wilkening (Tucson, AZ: Univ. Arizona Press), 341
Crovisier, J., Biver, N., Bockelée-Morvan, D., & Colom, P. 2009, P&SS, 57, 1162
Cruikshank, D. P., & Jones, T. J. 1977, Icar, 31, 427
Cutri, R. M., Wright, E. L., Conrow, T., et al. 2011, Explanatory Supplement to the *WISE* Preliminary Data Release Products, 1
Cutri, R. M., Wright, E. L., Conrow, T., et al. 2012, Explanatory Supplement to the *WISE* All-Sky Data Release Products, 1
Dello Russo, N., Vervack, R. J., Jr., Weaver, H. A., et al. 2008, ApJ, 680, 793
Fernández, Y. R. 1999, PhD thesis, Univ. Maryland
Fernández, Y. R., Kelley, M. S., Lamy, P. L., et al. 2013, Icar, 226, 1138
Finson, M. J., & Probstein, R. F. 1968, ApJ, 154, 327
Gehrz, R. D., & Ney, E. P. 1992, Icar, 100, 162
Harris, A. W. 1998, Icar, 131, 291
Hayward, T. L., Hanner, M. S., & Sekanina, Z. 2000, ApJ, 538, 428
Hillman, Y., & Prialnik, D. 2012, Icar, 221, 147
Holmes, E. 1892, Obs, 15, 441
Hsieh, H. H., Fitzsimmons, A., Joshi, Y., Christian, D., & Pollacco, D. L. 2010, MNRAS, 407, 1784
Ishiguro, M., Kim, Y., Kim, J., et al. 2013, ApJ, 778, 19
Ishiguro, M., Watanabe, J.-i., Sarugaku, Y., et al. 2010, ApJ, 714, 1324
Jarrett, T. H., Masci, F., Tsai, C. W., et al. 2013, AJ, 145, 6
Jewitt, D. 1991, in IAU Colloq. 116, Comets in the Post-Halley Era, Vol. 167, ed. R. Newburn, M. Neugebauer, & J. Rahe (Dordrecht: Kluwer), 19
Kossacki, K. J., & Szutowicz, S. 2010, Icar, 207, 320
Kossacki, K. J., & Szutowicz, S. 2011, Icar, 212, 847
Lacerda, P., & Jewitt, D. 2012, ApJL, 760, L2
Lamy, P. L., Toth, I., Fernández, Y. R., & Weaver, H. A. 2004, in Comets II, ed. M. C. Festou, H. U. Keller, & H. A. Weaver (Tucson, AZ: Univ. Arizona Press), 223
Lamy, P. L., Toth, I., Weaver, H. A., A'Hearn, M. F., & Jorda, L. 2009, A&A, 508, 1045
Lebofsky, L. A., Sykes, M. V., Tedesco, E. F., et al. 1986, Icar, 68, 239
Li, J., Jewitt, D., Clover, J. M., & Jackson, B. V. 2011, ApJ, 728, 31
Lin, Z.-Y., Lin, C.-S., Ip, W.-H., & Lara, L. M. 2009, AJ, 138, 625
Lisse, C. M., A'Hearn, M. F., Hauser, M. G., et al. 1998, ApJ, 496, 971
Lisse, C. M., Fernández, Y. R., Kundu, A., et al. 1999, Icar, 140, 189
Mainzer, A., Grav, T., Masiero, J., et al. 2011, ApJ, 736, 100
Masci, F. J., & Fowler, J. W. 2009, in ASP Conf. Ser. 411, Astronomical Data Analysis Software and Systems XVIII, ed. D. A. Bohlender, D. Durand, & P. Dowler (San Francisco, CA: ASP), 67
Min, M., Hovenier, J. W., de Koter, A., Waters, L. B. F. M., & Dominik, C. 2005, Icar, 179, 158
Montalto, M., Riffeser, A., Hopp, U., Wilke, S., & Carraro, G. 2008, A&A, 479, L45
Nelson, R. M., Soderblom, L. A., & Hapke, B. W. 2004, Icar, 167, 37
Reach, W. T., Vaubaillon, J., Lisse, C. M., Holloway, M., & Rho, J. 2010, Icar, 208, 276
Schleicher, D. G. 2009, AJ, 138, 1062
Sekanina, Z. 2008, ICQ, 30, 3
Sekanina, Z. 2009, ICQ, 31, 99
Sekanina, Z., Chodas, P. W., & Yeomans, D. K. 1998, P&SS, 46, 21
Sekanina, Z., Hanner, M. S., Jessberger, E. K., & Fomenkova, M. N. 2001, in Interplanetary Dust, ed. E. Grün, B.A.S. Gustafson, S. Dermott, & H. Fechtig (Astronomy and Astrophysics Library, Vol. 804; Berlin: Springer), 95
Sekanina, Z., & Yeomans, D. K. 1985, AJ, 90, 2335
Snodgrass, C., Lowry, S. C., & Fitzsimmons, A. 2006, MNRAS, 373, 1590
Soderblom, L. A., Becker, T. L., Bennett, G., et al. 2002, Sci, 296, 1087
Stevenson, R., & Jewitt, D. 2012, AJ, 144, 138
Stevenson, R., Kleyna, J., & Jewitt, D. 2010, AJ, 139, 2230
Sykes, M. V., Lien, D. J., & Walker, R. G. 1990, Icar, 86, 236
Tokunaga, A. T., Golisch, W. F., Griep, D. M., Kaminski, C. D., & Hanner, M. S. 1988, AJ, 96, 1971
Watanabe, J.-I., Honda, M., Ishiguro, M., et al. 2009, PASJ, 61, 679
Wright, E. L., Eisenhardt, P. R. M., Mainzer, A. K., et al. 2010, AJ, 140, 1868
Yang, B., Jewitt, D., & Bus, S. J. 2009, AJ, 137, 4538